

Digital blood image processing and fuzzy clustering for detection and classification of atypical lymphoid B cells

Edwin S Alférez², Anna Merino¹, Luis E Mújica², Magda Ruiz², Laura Bigorra¹, José Rodellar²

08036, 934 13 74 98, FAX: 93 413 74 0, santiago.alferez@upc.edu

¹*Servei d'Hemoterapia-Hemostasia. Centre de Diagnòstic Biomèdic. Hospital Clínic de Barcelona. Spain.* ²*Universitat Politècnica de Catalunya. Spain*

Abstract

Automated systems for digital peripheral blood (PB) cell analysis operate most effectively in non-pathological samples. The paper deals with the automatic classification of atypical lymphoid cells using digital image processing. The problem has been approached through a 3-step procedure: 1) Watershed segmentation of nucleus, cytoplasm and peripheral cell zone; 2) feature extraction for each region; and 3) classification using fuzzy c-means. The paper has proposed a new methodology that has been able to automatically classify with high precision three types of lymphoid cells: normal, Hairy Cell Leukemia cells and Chronic Lymphocytic Leukemia cells. This methodology, combining human medical expertise with mathematical and engineering tools, may contribute to improve the efficiency of the hematology laboratory.

Keywords: Digital Image Processing, Peripheral Blood, Hematology, Lymphoma.

1. Introduction

Peripheral blood (PB) is an organic fluid easily accessible and their study is the initial analytical step in the diagnosis of most of the hematological and non hematological diseases [1]. Frequently, the blood smear provides the primary or the only evidence of a specific diagnosis, remaining an important diagnostic tool even in the age of molecular analysis [2]. Morphological evaluation of leukemia and lymphoma cells is essential for diagnosis and classification. In the World Health Organization (WHO) classification, atypical cell morphology, along with immunophenotype and genetic changes, remains essential in defining lymphoid neoplasms [3].

Despite the significant improvements during the last years concerning to hematology analyzers, no significant progress has been made in terms of automatic classification of atypical PB cells. These devices are limited to identifying normally circulating leukocytes and flagging abnormal cells, without being able to classify the abnormal leukocytes [4].

Microscopy automation should be available in hematology laboratories. Developing of new innovative techniques in hematology laboratories, limitation of human resources and the complexity of pathologies create a need for automation in PB cytology. Furthermore, the close collaboration between cytologists, mathematicians and engineers over the last few years has made possible the development of automatic methodologies for digital image processing of normal blood cells. Some researchers have developed equipment that preclassify cells in different categories applying Neural Networks, extracting a large number of measurements and parameters which describe the most interesting cell morphological characteristics [4]. These automated systems integrated into the daily routine represent an interesting technological advance since they are able to preclassify most of the normal blood cells in PB [5].

Atypical lymphoid cells are the most difficult pathological cells to classify using morphology features [6]. For this reason few studies with satisfactory results have been published. They apply different methods of digital image processing to identify the atypical PB lymphoid cells in patients

with malignant lymphoid hematological diseases [7]. Moreover, the lymphoid cell classification has been addressed with pattern recognition systems in order to classify the cells in categories [8], [9], [10]. Although these studies showed good segmentation and description results, they did not apply subsequent biomedical studies to highlight its practical usefulness for the discrimination among different groups of similar diagnosis.

CLL cells are described as typically small lymphocytes with clumped chromatin and scant cytoplasm. HCL cells are larger than normal lymphocytes and they have abundant weakly basophilic cytoplasm with irregular “hairy” margins. Morphological distinction between various types of lymphoid cells requires experience and skill and do not exist objective values to define cytological variables.

In this paper we show a new methodology for lymphocyte recognition to improve the automatic classification of abnormal lymphoid cells circulating in PB in some B lymphoid neoplasms, such as CLL cells and hairy cells.

2. Material and methods

2.1 Blood sample preparation and digital image acquisition

Samples from patients with HCL and CLL were included in the study. The diagnoses were established by clinical and morphological findings as well as, characteristic immunophenotype of the lymphoid cells. Specifically CLL cells had the phenotype CD5+, CD19+, CD23+, CD25+, weak CD20+, CD10-, FMC7- and dim surface immunoglobulin (sIg) expression. All the patients with HCL had lymphoid cells with the phenotype CD11c+, CD25+, FMC7+, CD103+ and CD123+. Blood samples were obtained from the routine workload of the Core Laboratory of the Hospital Clínic of Barcelona. Venous blood was collected into tubes containing K3EDTA as anticoagulant. The samples were stored at room temperature and analyzed by a cell counter (Advia 2120, Siemens Healthcare Diagnosis, Deerfield, USA) and PB films were automatically stained with May-Grünwald-Giemsa in the SP1000i (Sysmex, Japan, Kobe) within 4 hours of blood collection.

The quality of the smears and cell morphology was assessed by hematologists prior to the image study. We selected 340 lymphoid cell images from PB films, where 90 images were lymphocytes from healthy patients, 100 were lymphoid cells from patients with HCL and 150 were lymphoid cells from patients with CLL. Each individual cell image had a resolution of 367 x 360 pixels and they were obtained by the CellaVision DM96 system.

2.2 Novel method for lymphocyte recognition

In this study we developed a novel method for lymphocyte recognition based on three steps:

- 1) Color segmentation of lymphoid cells. The goal of the segmentation procedure is to separate lymphoid cells from other objects in the image. The nucleus and the cytoplasm of each lymphocyte were segmented by two different procedures.
- 2) Feature extraction, which plays an important role in the leukocyte discrimination. From the previous segmentation step, 44 descriptors were selected. Some of them were visually comprehensible, such as the geometrical features (size, nucleus-cytoplasm ratio, nucleus eccentricity), but most of them were related with the texture features and derived from statistical properties. A new descriptor was introduced for the most interesting morphological characteristic of the hairy cells: the cytoplasmic profile feature.
- 3) Classification of the different lymphoid cells. We applied unsupervised Fuzzy C-mean (FCM) techniques for the classification of images in normal lymphoid cells and two types of atypical lymphoid cells: HLC and CLL cells.

2.3. Color Segmentation

A digital blood image is composed of a finite number of pixels. Each one has a particular location and color value, which can be represented in several spectral components or color spaces: RGB, HSV, among others. The primary RGB space corresponds to red, green and blue components and it is based on the Cartesian coordinate system. The HSV space corresponds to hue, saturation and brightness value. It is based on the representation of the color value over the cylindrical coordinate system. From the Cartesian coordinate system a new space color called “*Lab*” can be obtained, where *L* denotes lightness and *a* and *b* are the color-opponent dimensions. Unlike other color spaces, this new space includes all perceivable colors. Moreover, the objects are defined as each set of information from the image using the color space and/or mathematical procedures. Similarly, the color value of each pixel can be analyzed by its intensity information, which varies gradually from black to white. It is commonly known as gray scale [11].

Two segmentation procedures were implemented alternatively in order to identify the objects from each cell image.

2.3.1 Segmentation by Active Contours

This method recognizes the cellular components by using the color information from the original image. Applying the active contours technique (AC) [12], [13] on the H component of HSV color space, the entire cell can be obtained. Likewise, the entire nucleus is also obtained but using RGB color space [14].

2.3.2 Segmentation method using Watershed Transformation

A grey-level image might be seen as a topographic relief. The concept of Watershed transformation (WT) is based on visualizing the maximum and minimum intensity values as peaks and basins. Then, water falling on this relief flows to reach a minimum. Intuitively, the watershed of a relief corresponds to the limits of the adjacent basins of the water regions [15].

In this work, the WT was applied only on the gradient of the green component from RGB color space. Since the gradient highlights the edges (high intensity changes) of the objects, we included some external and internal markers as minimum values over the gradient image in order to improve the delimitation of the different regions. Thereby, the over-segmentation was avoided and only the entire lymphoid cell is separated. Once the entire lymphoid cell was separated, new markers were imposed and the WT was applied again to segment the nucleus.

Afterwards, mathematical morphology operations were done in order to improve the quality of the regions from the nucleus and cytoplasm. Finally, three different regions of the cell were identified: the cytoplasm, the nucleus and the peripheral zone around the cell.

2.4. Feature Extraction

The feature extraction is a stage that obtains information about objects in the image to be analyzed. The features that may be calculated depend on both qualitative and quantitative reasoning, i.e., ideas or concepts that might be abstracted from the expert (converted to quantitative values). The evaluation of mathematical descriptors could provide more information about morphological parameters, but they are not easily interpreted. Table 1 shows a list of all 44 features used in this work: 10 geometric, 30 texture features, three related with basophilia intensity, and one related with the external profile of the cytoplasm. The values of these features for each image cell were stored in a matrix of dimension 340 x 44.

2.4.1 Geometric Features

These features are geometric interpretations of the cell and nucleus shape. For each cell and nucleus, the “Areas”, “Diameters” and “Perimeters” were calculated using the regions of the cell.

Equally, the “Conic eccentricities”, which determine the cell and nucleus roundness, were calculated. The “Nucleus – cytoplasm ratio” was calculated by dividing the respective areas. The “Nucleus eccentricity relative to the cell center” was calculated as the distance between the center of the cell and the nucleus [16].

Table 1. A set of 44 features for their extraction: 1 from the external profile of the cytoplasm, 10 geometrical features, 30 texture features and 3 from basophilia intensity.

Kind of Feature	Quantitative Feature	
Cytoplasmic profile feature	(1) Estimation of the Hairy projections	
Geometrical features	(2) Cell area	(3) Cell diameter
	(4) Cell conic eccentricity	(5) Cell perimeter
	(6) Nucleus area	(7) Nucleus diameter
	(8) Nucleus conic eccentricity	(9) Nucleus perimeter
	(10) Nucleus – cytoplasm ratio	
	(11) Nucleus eccentricity respect to the cytoplasm	
	Cytoplasm	Nucleus
First-order statistical features	(12) Mean	(25) Mean
	(13) Standard Deviation	(26) Standard Deviation
	(14) Skewness	(27) Skewness
	(15) Kurtosis	(28) Kurtosis
	(16) Energy	(29) Energy
	(17) Entropy	(30) Entropy
Second-order statistical features	(18) Contrast	(31) Contrast
	(19) Homogeneity	(32) Homogeneity
	(20) Correlation	(33) Correlation
	(21) Energy	(34) Energy
	(22) Entropy	(35) Entropy
	(23) Variance	(36) Variance
	(24) Difference Variance	(37) Difference Variance
Granulometrical features (based on granulometrical curve)		(38) Mean
		(39) Standard Deviation
		(40) Skewness
Basophilia		(41) Kurtosis
	(42) Mean of <i>L</i> color	
	(43) Mean of <i>a</i> color	
	(44) Mean of <i>b</i> color	

2.4.2 Texture Features

Several statistical measures were used to describe the texture of the cytoplasm and nucleus regions [17]. They were organized in two groups: first and second order statistical features, respectively. The first group was based on the histogram of the image. The histogram shows the number of pixels with each specific value. Then, the Skewness measures the asymmetry of the shape; the Kurtosis, the relative flatness; the Energy, the uniformity; and the Entropy, the variability. In addition, the Mean and the Standard Deviation were calculated.

The second-order statistical features can be calculated using the co-occurrence matrix for each region. In this way, information about the position and the intensity of the pixels can be obtained [18]. In this work the following features were considered: Contrast, Homogeneity, Correlation, Energy, Entropy and Difference Variance. Additionally, these descriptors contribute with more information from the images.

2.4.3 Granulometrical features of the nucleus

The granulometry estimates the size distribution of the bright and dark spots on the image. Identifying and counting these spots directly on the image is usually a complicated procedure. For this reason, gray scale mathematical morphology (opening and closing) [11] is used to estimate indirectly the size distribution of them by the sums of intensities of the processed images. It leads

to the Granulometric Curve, which places the information from the dark spots on the left (negative coordinates) and the information from the bright spots on the right (positive coordinates) [19]. Consequently, from the granulometric curve of the lymphoid cell, we calculated four features: mean standard deviation, skewness and kurtosis, in order to discriminate the different types of nuclear texture and improve chromatin description.

2.4.4 Basophilia features of the cytoplasm

Cytoplasmic basophilia can be estimated by color analysis. The Lab color space is characterized by its approximation to human perception. Therefore, the means of the intensities in each color component are convenient to represent the basophilia degree of the cytoplasm [16].

2.4.5 Cytoplasmic profile feature

In this paper we propose a novel method to characterize the cytoplasmic profile. It estimates the projections of the cytoplasm using the peripheral region around the cell segmented by WT. This feature is obtained by using thresholding segmentation to the green component and counting the pixels of this region.

2.5 Classification

Once the features of each cell were calculated, the next step was to use them to classify the lymphoid cells into the three different groups included in this work: normal cells (N), hairy cells (HCL) and chronic lymphocytic leukemia cells (CLL).

As it was explained in Section 2, all features were stored in a matrix. Each vector row corresponds to the set of features of each cell and it was used as the input data for the classification. For this, the clustering algorithm Fuzzy C-means (FCM) was applied. Similar input data were grouped in each cluster with certain membership degree [20]. Finally, the maximum membership value was considered to select the cluster for each lymphoid cell.

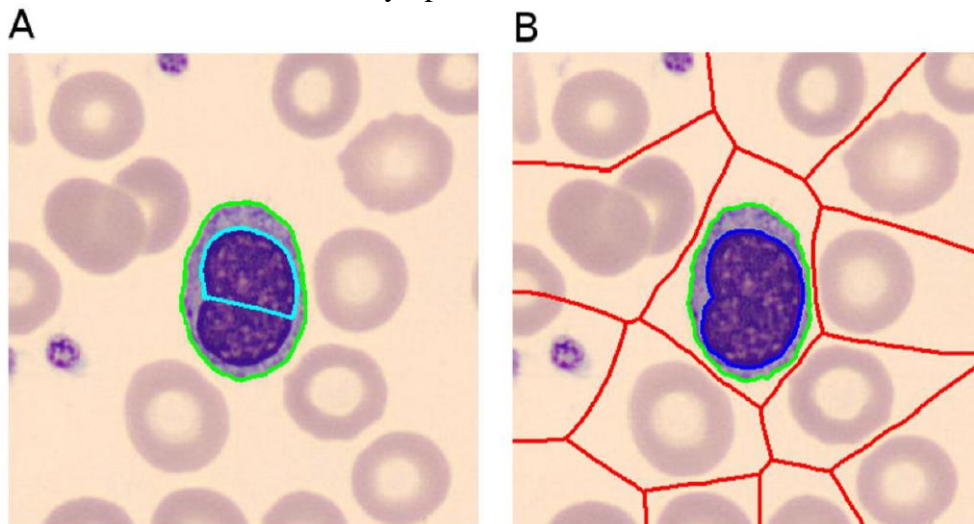


Figure 1. An example of segmented cells: using active contours segmentation two regions are obtained (A), while using Watershed segmentation three regions are found: nucleus, cytoplasm and peripheral zone of the cell (B).

3. Results

Segmentation is a crucial part of the methodology. Two different segmentation procedures were implemented: Active Contours technique (AC) and Watershed Transformation (WT). AC reached a good efficiency to separate the outer profile of the cytoplasm. Nevertheless, the method was deficient to segment the nucleus because of their characteristic granular texture. In addition, the

computational cost was too high since the algorithm executes a huge amount of numerical operations. In contrast, WT was more effective separating the nucleus. Besides, it allowed segmenting more regions, specifically the outer profile of the cytoplasm, which is very important to extract the useful information to discriminate different types of lymphocytes. Moreover, its computational cost was low. Figure 1 shows two examples of segmented cells using both techniques. Using AC segmentation two regions were obtained (Figure 1A). In contrast, using WT segmentation three regions were found: nucleus, cytoplasm and peripheral zone of the cell (Figure 1B). In consequence, WT methodology was selected and applied to segment the lymphoid cell images selected in this work.

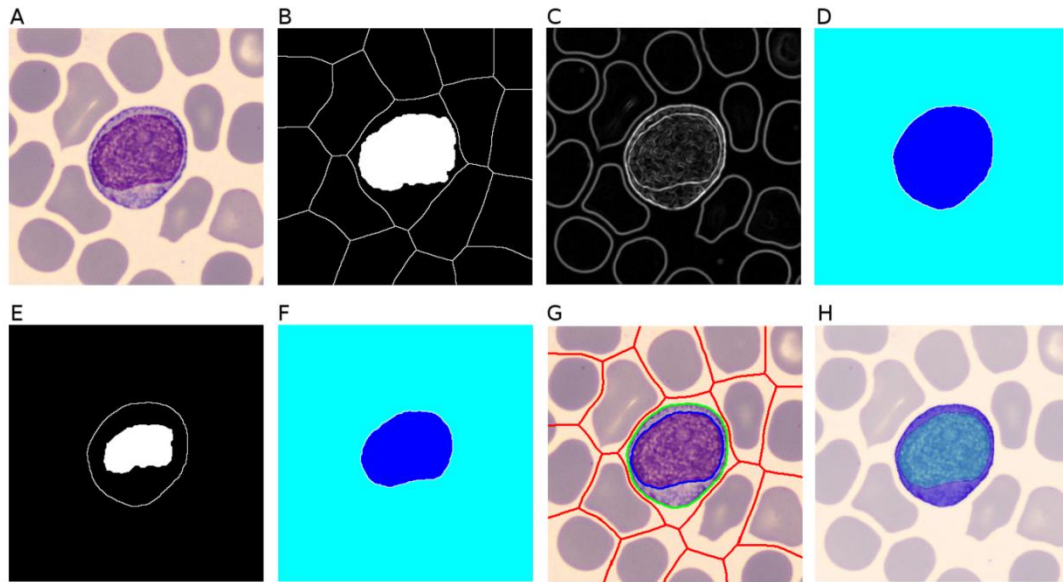


Figure 2. Images corresponding to the different stages of the Watershed segmentation (WT). The original cell (A) is processed to obtain the external and internal markers (B). The WT is calculated on the gradient of green component (C). The markers limit the WT to segment the cell (D). Once the lymphoid cell is separated its edges are used as the new external marker and the thinned mask of the nucleus as the new internal marker (E) in the WT to segment the nucleus (F). Finally the watershed lines (G) show the regions of interest: the nucleus, the cytoplasm (H) and the peripheral zone around the cell.

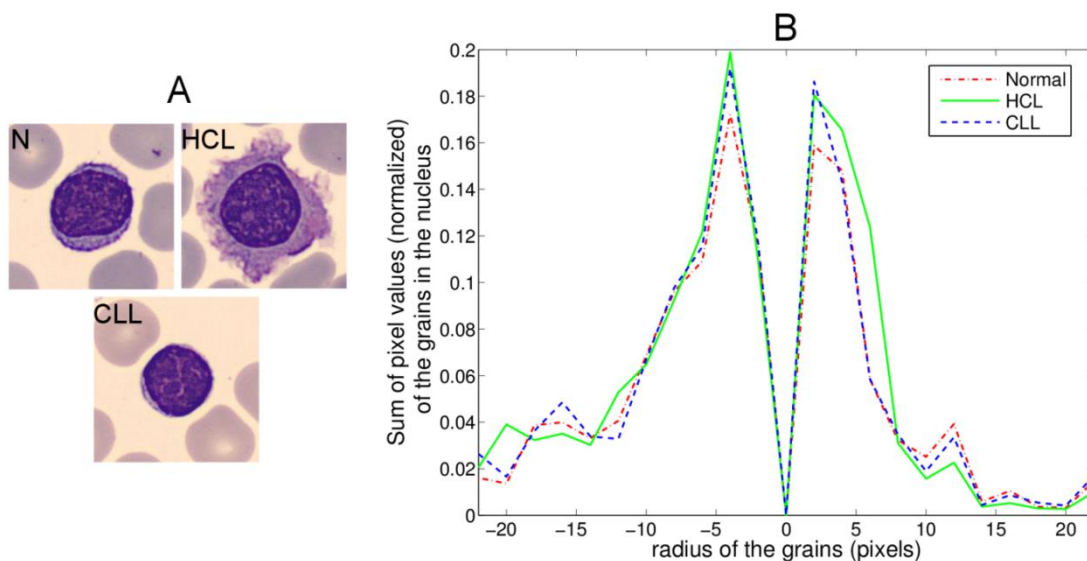


Figure 3. Normal (N), HCL and CLL lymphocytes (A) and their corresponding granulometric curves (B) which places the information from the dark spots on the left (negative coordinates) and the information from the bright spots on the right (positive coordinates).

Figure 2 shows the images corresponding to the different stages that we obtained applying the WT segmentation to the lymphoid cells. The lymphoid original cell stained with MGG is showed in Figure 2A. The WT was applied only on the gradient of the green component from RGB color space (Figure 2B). Since the gradient highlights the edges (high intensity changes) of the objects, some external and internal markers should be included as minimum values over the gradient image to improve the delimitation of the different regions as shown in Figure 2C. Thereby, the over-segmentation was avoided and only the entire lymphoid cell was separated (the darkest region on Figure 2D). Once the entire lymphoid cell was separated, new markers were imposed (Figure 2E) and the WT was applied again to segment the nucleus (Figure 2F).

Afterwards, mathematical morphology operations were performed in order to improve the quality of the regions from the nucleus and cytoplasm. Finally, three different regions of the cell were identified: the cytoplasm, the nucleus and the peripheral zone around the cell (Figures 2G and 2H).

Figure 3 shows an example of normal, HCL and CLL lymphoid cell images (Figure 3A) and their granulometrical curves. Figure 3B shows how these curves discriminate the types of nuclear texture in the different lymphoid cells, improving chromatin description. In order to obtain information from each curve, four features were calculated: mean, standard deviation, skewness and kurtosis.

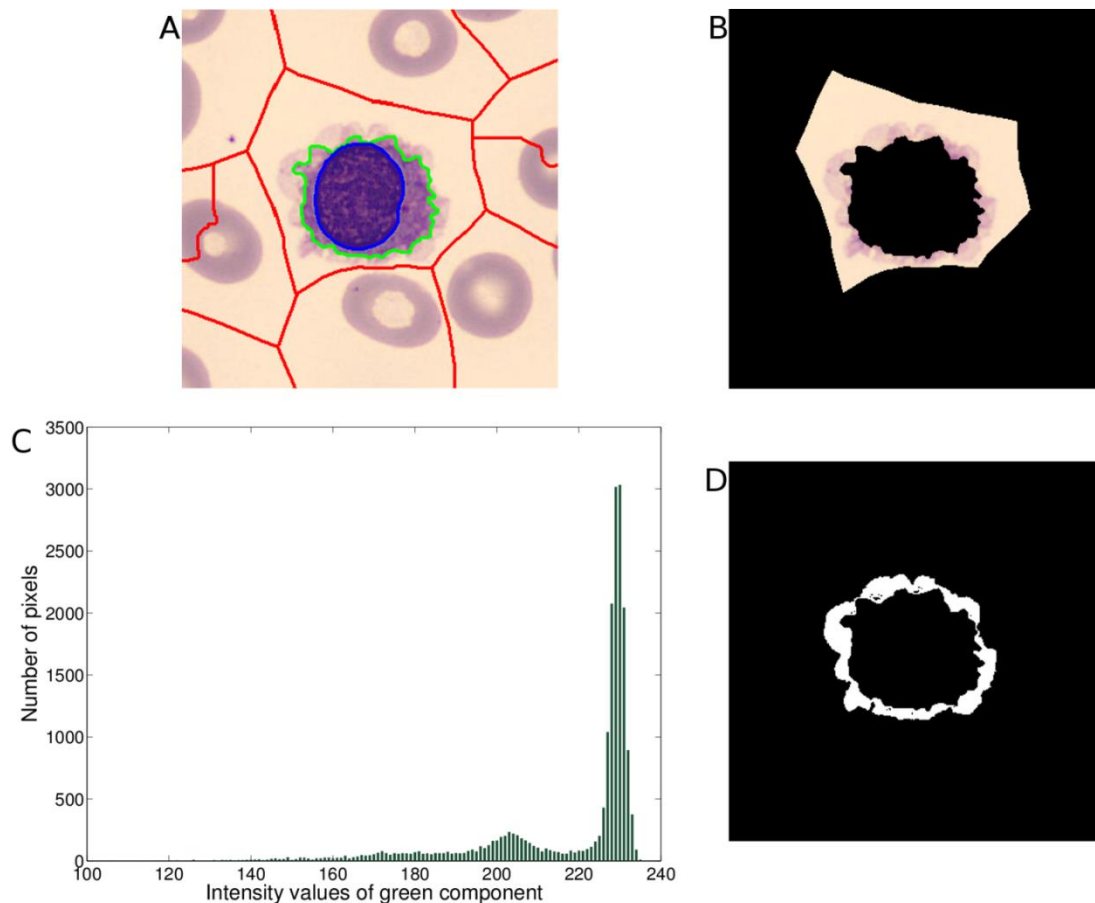


Figure 4. Stages to calculate the cytoplasmic feature corresponding to a HCL cell. After the cell segmentation (A), the peripheral zone around the cell was selected (B). The histogram representation of this region showed an intermediate lobe that contained most of the “hairy” projections (C). Then, the presence of these projections was determined (D). Finally, this area was quantified.

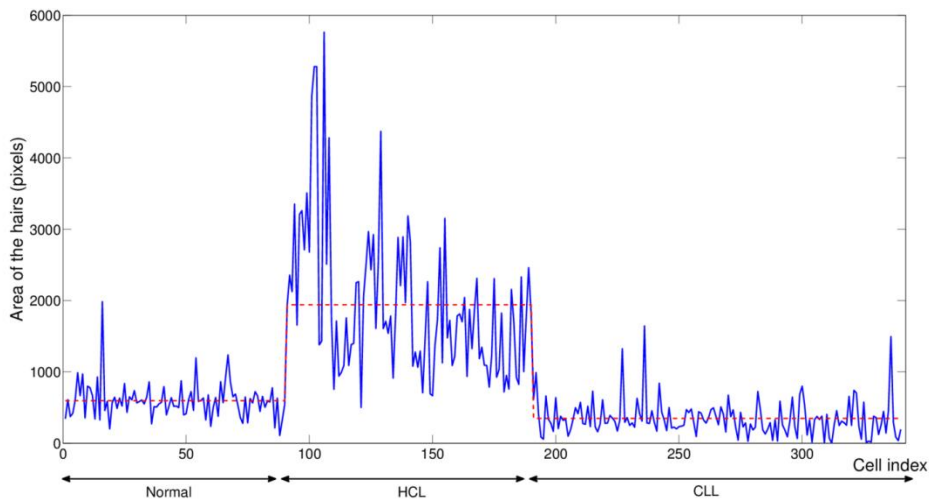


Figure 5. Cytoplasmic profile feature in normal, HCL and CLL lymphoid cells. HCL cells showed very high values of this feature compared with CLL and normal lymphoid cells

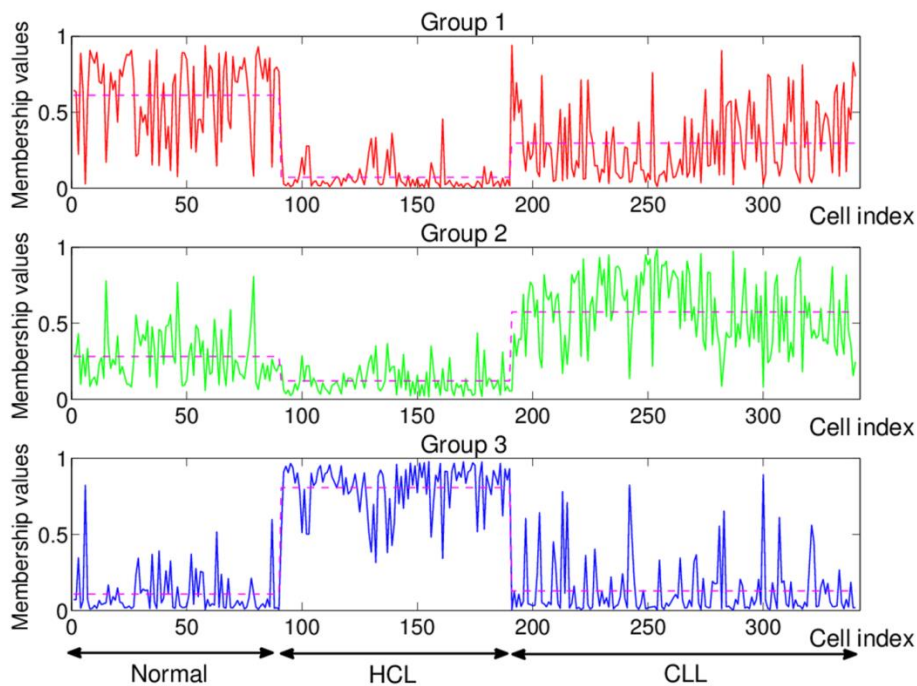


Figure 6. Membership function of each type of cell: normal lymphocytes (Normal), hairy cells (HCL) and lymphoid cells from chronic lymphocytic leukemia (CLL). The horizontal axis represent the cells, while the vertical axis represents the probability of belonging to each group. The horizontal line for each type of cell represents the mean of their membership values in each group.

Figure 4 displays the cytoplasmic profile feature extraction obtained in one of the hairy cell images. After the segmentation of the cell (Figure 4A), the peripheral zone around the cell was selected (Figure 4B). The histogram representation of this region showed an intermediate lobe that contained most of these “hairy” projections (Figure 4C). Then, the presence or absence of these projections was determined (Figure 4D). Finally, this area was quantified. The novel cytoplasmic profile feature proposed in this work was decisive for the detection of the hairy cells. Figure 5 shows the characteristic cytoplasmic profile feature for all the cells. HCL cells showed very high values of this feature compared with CLL and normal lymphoid cells.

Afterwards, the 44 features of the 340 available cells were used to create the data matrix. It was automatically clustered in three groups using FCM (first step), producing three membership functions. Since every cell pertains to one of the three groups with different degrees of membership, we used the criterion that each lymphoid cell belongs to the group with the highest membership value. The left part of Table 2 gives a summary of the whole data obtained in the first FCM classification step. This shows an excellent classification on the group 3 because it included 98% of the HCL cells. However, the groups 2 and 3 contained 75.6% of normal lymphoid cells and 62.7% of CLL cells, respectively. Figure 6 contains three plots corresponding to each group. The horizontal axis represents each individual cell, while the vertical axis gives its membership value. These three values represent the probability of belonging to each group, their sum being equal to 1. In every plot, the data set was sorted in this way: the first 90 images belong to normal lymphocytes, the following 100 to HCL cells and the last 150 to CLL cells. From Figure 6, it was clear to assure that both the normal cells and the CLL cells do not belong to group 3 due to their low membership values. It was also clear that HCL cells had high probability to belong to group 3. On the contrary, from Figure 6 it was difficult to infer to which group (1 or 2) belong the normal and the CLL cells due to the high variance of their membership values in groups 1 and 2.

In order to improve the classification, once the HCL group was identified the set of the remaining cells was clustered again using FCM (second step). In this new clustering process only two types were considered (N and CLL cells) and only the texture features were used. The right part of Table 2 gives a report of the results in this step: the percentages of normal lymphoid cells increased to 83.3 % in the new group 1 and the percentages of CLL cells increased to 71.3% in the new group 2. Figure 7 shows the membership values for these two new groups. In this case, it was clear enough to distinguish these two types of cells, because their membership values were quite different for a significant percentage of cells as observed in the right part of Table 2. The mean values were clearly different.

As a summary, Figure 8 shows schematically the complete classification methodology of the lymphoid cells using the FCM. First, three different groups of data were obtained and each group contained cells of the three types. Subsequently, in order to improve the classification in groups 1 and 2, a second FCM was applied using only the texture features. It resulted in two new groups: New Group 1 and New Group 2.

Table 2. *Classification in two steps. First, three different classes of data were obtained. Each group has cells of the three types, i.e. the group 3 has 98% of the HCL cells. A second FCM was applied using only the texture features. It resulted in two new groups with 83.3% of normal lymphoid cells and 71.83% of CLL cells, respectively.*

Type	FCM step 1			FCM step 2	
	Group 1	Group 2	Group 3	New group 1	New group 2
N	75.6 %	20 %	4.4 %	83.3 %	12.2 %
HCL	1 %	1 %	98 %	2 %	0%
CLL	30 %	62.7 %	7.3 %	21.3 %	71.3 %

4. Discussion

In this study, normal and two types of atypical lymphoid cells (HCL and CLL) have been analyzed using mathematical morphology for image processing and fuzzy clustering. These cells have distinctive geometrical, granulometry, basophilia and cytoplasmic profile features. HCL and CLL cells were selected in our work for their representative morphology and the large number of these cells that we obtained from the routine workload in our laboratory.

Cell morphology is subject to variability in slide making and staining procedures. In order to minimize this variability, the images used in this work were obtained in a standard and reproducible way using automatic staining and the Cellavision DM96 analyzer. The system scanned the slides identifying different types of white blood cells (WBC). It takes digital cell images and uses artificial neural network to analyze them [4], [5]. The analyzer preclassifies WBC but is not able to separate the different abnormal lymphoid cells circulating in PB in some B cell lymphoid neoplasms [21].

Since atypical lymphoid cells are the most difficult ones to classify using only morphology features [6], in this work a new methodology is proposed combining segmentation, feature extraction and classification algorithms. We demonstrated that this automated image-based methodology extracted granulometrical, basophilia and cytoplasmic profile features in an objective and reproducible way. Then, this methodology could provide a new generation of automated systems tool to assist in the diagnosis through hematological cytology.

Our results showed that texture descriptors were the most relevant in CLL lymphoid cell discrimination. Moreover, nuclear characteristic is an important feature in morphological diagnosis. The nuclear staining pattern reflects chromatin organizations and, in addition, the CLL cells typically contain clumped chromatin [22]. Therefore it supplies a good descriptor.

In a previous work, Angulo et. al. [16] used granulometry to describe cytoplasmic profile feature in six image cells. In this sense, in our work a novel cytoplasmic profile feature is proposed based on a simple thresholding of the peripheral zone around the cell. As we expected, this feature was crucial for the HCL cells detection since they show in PB stained with MGG a soft, blue-gray cytoplasm with hair-like cytoplasmic projections. On the other hand, this feature could be used for the detection of another atypical lymphoid cells with cytoplasmic villous, such as the splenic marginal zone lymphoma.

Concerning to the classification process, Sabino et. al. [23] used 26 features (geometrical and second-order statistical features) to automate the classical microscopic diagnosis, obtaining good results in the classification of CLL cells but only with respect to the different “normal” types of leucocytes from PB. In our work, 44 features are used adding other geometrical and second-order statistical features and also basophilia, granulometrical, first-order statistical features and cytoplasmic profile features. In addition, we distinguish three types of lymphoid cells: normal, CLL and HCL cells. It is relevant to remark that, up to our knowledge, hairy cells have never been automatically classified before.

The study presented in this paper has been performed to discriminate between three groups of lymphoid cells with encouraging results. The developed methodology can be extended to another classed of atypical lymphoid cells circulating in peripheral blood in some lymphoid neoplasms. We are progressing with further work in this direction. The overall goal is to combine medical, engineering and mathematical backgrounds to provide more objective and reproducible estimation of the lymphoid cell morphology than the standard microscopy analysis. The combination of automated tools with human medical expertise may contribute to improve the efficiency of a modern hematology laboratory.

5. Referencias

1. Houwen B. The differential cell count. *Lab Hematol* 2001;7:89-12.

2. Bain BJ. Diagnosis from the blood smear. *N Engl J Med* 2005;353:498-10.
3. Swerdlow SH, Campo E, Harris NL. WHO classification of tumours of haematopoietic and lymphoid tissues. France: IARC Press; 2008.
4. Ceelie H, Dinkelaar RB, van Gelder W, Examination of peripheral blood films using automated microscopy; evaluation of Diffmaster Octavia and Cellavision DM96. *J Clin Pathol* 2007;60:72-8.
5. Briggs C, Longair I, Slavik M, Thwaite K, Mills R, Thavaraja V, et al. Can automated blood film analysis replace the manual differential? An evaluation of the CellaVision DM96 automated image analysis system. *Int J Lab Hematol* 2009;31:48-13.
6. Gutiérrez G, Merino A, Domingo A, Jou JM, Reverter JC. EQAS for peripheral blood morphology in Spain: a 6-year experience. *Int J Lab Hematol* 2008;30:460-7.
7. Scotti F. Robust Segmentation and Measurements Techniques of White Cells in Blood Microscope Images. Instrumentation and Measurement Technology Conference, 2006. IMTC 2006. Proceedings of the IEEE 2006;43-6.
8. Bergmann M, Heyn H, Müller-Hermelink HK, Harms H, Aus HM. Automated recognition of cell images in high grade malignant lymphoma and reactive follicular hyperplasia. *Anal Cell Pathol* 1990;2:83-13.
9. Foran DJ, Comaniciu D, Meer P, Goodell LA. Computer-assisted discrimination among malignant lymphomas and leukemia using immunophenotyping, intelligent image repositories, and telemicroscopy. *IEEE Trans Inf Technol Biomed* 2000;4:265-9.
10. Juan J, Sigaux F, Flandrin G. Automated Classification of Lymphoid Cells. *Anal Quant Cytol* 1985;7:38-9.
11. Gonzalez RC, Woods RE. Digital image processing. Upper Saddle River, NJ: Prentice Hall;2008.
12. Xu C, Prince JL. Snakes, shapes, and gradient vector flow. *IEEE Trans Image Process* 1998;7:359-11.
13. Sadeghian F, Seman Z, Ramli AR, Abdul Kahar BH, Saripan M-I. A framework for white blood cell segmentation in microscopic blood images using digital image processing. *Biol Proced Online* 2009;11:196-11.
14. Alférez E, Merino A, Mujica L, Rodellar J, Morphological features using digital image processing in lymphoid neoplasias [Abstract]. *Int J Lab Hematol* 2011;33 Suppl:53 -1.
15. Beucher S, Meyer F. The morphological approach to segmentation: the watershed transformation. In Dougherty E, ed. *Mathematical morphology in image processing*. New York: Marcel Dekker 1992: 433-49.
16. Angulo J, Klossa J, Flandrin G. Ontology-based lymphocyte population description using mathematical morphology on colour blood images. *Cell Mol Biol* 2006;52:3-14.
17. Materka A, Strzeleck M, Texture analysis methods - a review. Technical university of lodz, institute of electronics, COST B11 report, Brussels, 1998. Available from: http://www.eletel.p.lodz.pl/programy/cost/pdf_1.pdf
18. Haralick RM, Shanmugan K, Dinstein I, Textural features for image classification, *IEEE Trans Syst Man Cybern* 1973;3:610-12.
19. Angulo J. A mathematical morphology approach to the analysis of the shape of cells. In Bonilla LL, Moscoso M, Platero G, Vega JM, eds. *Progress in Industrial Mathematics at ECMI 2006*. Leganes, Spain: Springer 2006:543-5.
20. Pal NR, Bezdek JC. On cluster validity for the fuzzy c-means model. *IEEE Trans Fuzzy Syst* 1995;3:370-10.
21. Merino A, Bruges R, Garcia R, Kinder M, Bedini JL, Escolar G. Comparative study of peripheral blood morphology by conventional microscopy and Cellavision DM96 in hematological and non hematological diseases [Abstract]. *Int J Lab Hematol* 2011;33 Suppl:112 -1.
22. Jahanmehr SH, Rogers M, Zheng J, Lai R, Wang C. Quantitation of cytological parameters of malignant lymphocytes using computerized image analysis. *Int J Lab Hematol* 2008;30:278-8.

23. Sabino DMU, Da Fontoura Costa L, Rizzatti EG, Zago MA, A texture approach to leukocyte recognition, *Real-Time Imaging* 2004;10:205-12.
24. Summers TA, Jaffe ES. Hairy cell leukemia diagnostic criteria and differential diagnosis. *Leuk Lymphoma* 2011;52:6-5.